EXPERIMENTAL INVESTIGATION INTO THE HYDRODYNAMICS EFFECTS OF SLOT FILM COOLING ON A CYLINDRICAL MODEL

E. Esmaeilzadeh

Department of Mechanical Engineering
University of Tabriz
Tabriz, Iran

Abstract An experimental study of hydrodynamics of *film cooling* is performed by using a single longitudinal slot on a cylindrical model simulated to the leading edge of the gas turbine blade. The model is set up into the test section of an open-cricuit induced flow wind tunnel which provides the main flow. The injected air, as a secondary film flow, produced from a high pressure compressor is considered so that, the cooling factor always remained between 0.1 and 3.9. The first separation region of the boundary layer over the cylinder caused by the presence of injected flow was determined. The separation region extends up to 20 degrees after injection point with different conditions used in this experiment.

Key Words Gas Turbine Blade, Leading Edge, Film Cooling, Slot Film Cooling, Cooling Factor, Effectiveness of Film Cooling

چکیده بررسی تجربی هیدرودینامیک خنک کاری لایه‌ای شیاری (slot film cooling) با استفاده از شیار طولی روی مدل استوانه ای بعنوان مدل ناحیه لبه حمله پره یک توربین گازی، مورد توجه است. مدل در مقطع کار تونل باد مادون صوت بازی که جریان اصلی را ایجاد می کند، بطور افقی نصب شده است. جریان تزریق هوا، بعنوان جریان ثانوی لایه ای توسط کمپرسور فشار قوی ایجاد می شود تغییرات فاکتور خنک کاری (cooling factor) در محدوده (۳/۹،۰/۱) مورد نظر است. جدایش اولیه لایه مرزی از روی استوانه در اثر حضور جریان تزریقی، مشاهده شده است. وسعت ناحیه جدایش اولیه (FSR) لایه مرزی با توجه به شرایط تجربی در این کار، از شیار تزریق شروع و تا محدوده ۲۰ درجه بعد از آن قرار می گیرد.

INTRODUCTION

Gas turbine is used as an energy generating device in thermal power plants and air craft engines for many years. During this period its efficiency has been considerably improved.

In principle, it is possible to improve the efficiency be increasing the turbine inlet temperature. In the power plant applications this temperature is normally arround 900°C; and recently it has been raised up to 1200°C [1]. However, due to the metallurgical and thermal stress limitations, it is not possible to increase this temperature to a great extent. Barry has shown [2] that, if these limits are increased or decreased by 20°C, the life time of the blades will become one half and twice of the ordinary ones respectively. Many attempts have been made to replace the common alloys by the new materials, but in some cases the afforts have led to the models which are not economically suitable.

Parallel to these works, many atempts have been made to raise the inlet temperature by preventing the direct contact of hot stream gas with the solid wall; this has been done by a secondary injected flow used as a protecting layer. For this purpose, the film cooling methods have been considered for many year; but because of theoretical complexities, most of works have been based on the experiments for simple

geometries. Of course some theoretical and numerical treatments have been carried out [3-6].

In general, the injection cooling methods may be classified into the transpiration cooling and film cooling. In the film cooling, they use holes and slots for injection. Many available works mostly use the flat surfaces for the moderate pressure gradients [7-9]. There are few analyses in which the strong pressure gradients have been considered [10, 11, 16].

In a gas turbine, the film cooling method has been widely used. In principle, because of its undesirable effects on the aerodynamic and thermodynamic efficiencies, the mass flow rates of injection should be less than 4% of the main flow rates [6]. There are several methods to inject secondary flow into the main stream and it is not possible to find out a general procedure which can predict all aspects of film cooling phenomena from both theoretical and experimental perspectives. Even if only one blade of a gas turbine is used to study the film cooling phenomenon, it is really impossible to predict the problems, when two shear layers interact.

As shown in Figure 1, the distribution of Nusselt number is not uniform on the surface of gas turbine blade [6].

Figure 1 indicates that the leading edge region has a very high Nusselt number, and because of heat transfer rates it should be protected first from direct contact of hot gas flows. This region, in most gas turbine blades, is geometrically a part of circular cylinder. Obviously in this case, the phenomena will be more complex than that of the flat case due to presence of the pressure gradients.

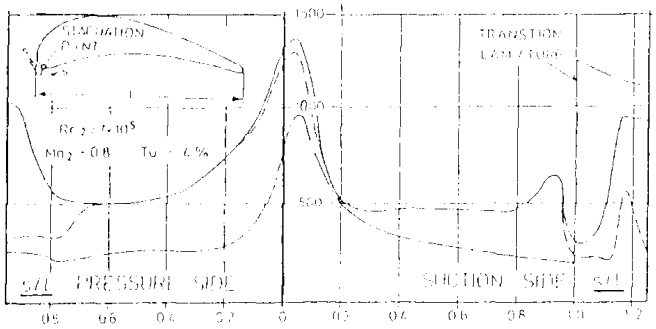

——— Theoretical
——— Experimental
– – – – Experimental (Analysis includes radiant heat transfer)

Figure 1. Distribution of Nusselt number over a gas turbine blade [6].

The foregoing considerations have served to motivate the present investigation. The cylindrical model is taken and in order to simplify the model, a single longitudinal slot parallel to the axis of the cylinder is used for a two-dimensional injection study.

The effectiveness of film cooling for constant properties of two shear flows is defined as:

$$\eta = \frac{T_{aw} - T_\infty}{T_i - T_\infty}$$

where T_{aw} is the adiabatic wall temperature, T_∞ is the main temperature, T_i is the injected fluid temperature and η is the local adiabatic film cooling efficiency or its *effectiveness*. For a better understanding of the phenomena, in addition to the hydrodynamics investigation, the heat transfer experiments must be carried out.

EXPERIMENTAL APPARATUS AND PROCEDURE

Two fluid flows were considered with constant physical properties. Their mass flux ratios or the *cooling factor*, ($M = \rho_i V_i / \rho_\infty V_\infty$), have been taken in the range of $0.1 < M < 4$.

The schematic representation illustrated in Figures 2 and 3 respectively. The apparatus has two main parts, the first one is an open circuit subsonic wind tunnel which provides the main flow. The test section of the wind tunnel was made by a plexiglas material and its dimensions are 308 mm × 308 mm × 450 mm. The main velocity in wind tunnel was measured by means of a pitot-static tube. The static pressures

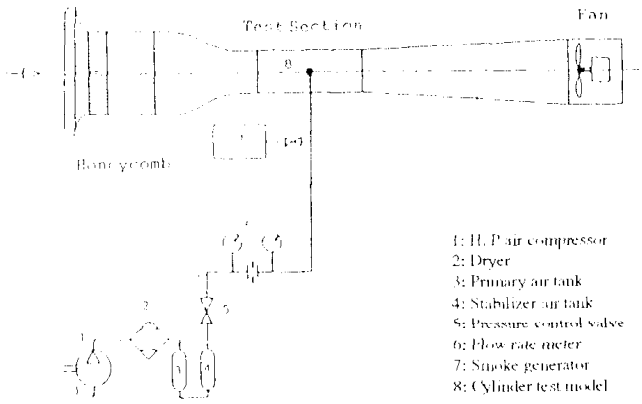

Figure 2. A schematic presentation of the experimental apparts.

along the circumference section of the model were obtained by using a multi manometer which was connected to the eighteen static pressure tap holes located 10 degrees apart around circumference of the middle section of the cylinder. The second part of the apparatus produces the secondary air flow. For this purpose, the high pressure compressor was used. This compressor, with maximum 20 bars and 12.5 m^3/s capacity, is equipped with a dryer and two big tanks (each has a volume of $3m^3$). Therefore, its

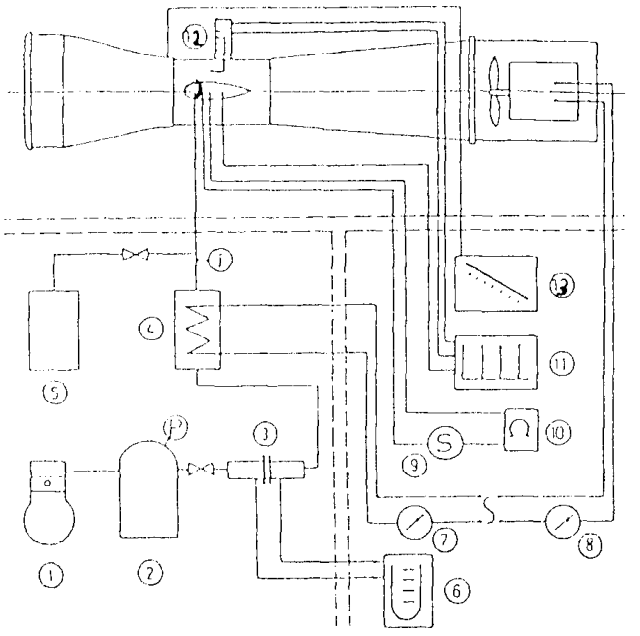

1-HP COMPRESSOR 2-PRIMERY & SECONDARY TANKS 3-FLOW METER 4- HEATER 5- SMOKE GENERATOR 6- MANOMETER 7- HEATER CONTROLLER 8- FAN SPEED CONTROLLER 9- N. T. C. SELECTROR FOR EFFECTIVENESS MEASURMENTS 10- DIGITAL AMMETER 11- MULTIMANOMETER 12- PITOT TURE 13- MICROMANOMETER.

Figure 3. Experimental set up

vibration and istability can not affect the secondary flow. The pressure of the compressed air from the second pressure vessel is adjusted and entered the injection line of experimental apparatus. The injection line involves one orifice flow rate meter wherein the secondary flow was measured. The flow can also be visualized using a special smoke generator introduced in the injection line.

The expreimental model is a 50 mm diameter and 308 mm long cylinder. It was set up horizontally in the test section. To inject the secondary flow, a 2.5 mm width wide and 230 mm length longitudinal slot parallel to the axis of the model was made on the surface of the cylinder.

The secondary mass flow rate was measured by an orifice flowmeter based on the french norm of standard with specification number NF X10 - 102. The mass flow rate is obtained by the following formula:

$$m^{\circ} = \varepsilon\, \alpha [2\, \rho\, (P_1 - P_2) / (1 - \beta^4)]^{1/2}$$

with,

$$\alpha = A + B\, (10^6 / R_{eD})^{1/2}$$

$$\beta = d / D \; ; \; R_{eD} = D.V.\rho / \mu$$

$$A = 0.592 + 0.425[0.387/(D^2.\beta^2 + 0.254\ D) + \beta^4 + 1.25\ \beta^{16}]$$

$$B = 0.0025 + 0.00235[\beta + 1.75\beta^4 + 10\beta^{12} + 0.078\ D\ \beta^{16}]$$

wherein; P_1 and P_2 denote pressures before and after orifice respectively, d diameter of orifice and D diameter of the pipe. The effect of compressibility of air flow has been considered by the coefficient of ε as follows:

$$\varepsilon = 1 - (0.41 + 0.35\ \beta^4)\ ((P_1 - P_2)/P_1)$$

The uncertainty analysis of the mass flow rate which

was used for determining the cooling factor, was obtained with the relative error of m° as:

$$\Delta m^\circ / m^\circ = 3/2\ \Delta h / h$$

where h represents the difference in pressure which was measured by means of a simple U type differential manometer. Regarding the experimental running, the relative errors of injected velocity, V_i, become around 1%. The same analysis for V_∞, shows the relative errors less than 2.5%. Therefore, the value of the film cooling factor, M, was obtained within $\mp 3\%$.

The secondary flow enters a 16 mm diameter and 400 mm long brass cylinder insert, used a distributor. This insert was designed to fit inside the main cylinder. It has 4 rows holes in staggered arrangement with 5 mm diamter. The two dimensional jet issuing from the slot of the model had been approved by the experimental results when the main flow was absent that is, the uniform distribution of the injected two dimensional flow in the length of slot was obtained. In Figure 4 the schematic representation of the model and its details are shown.

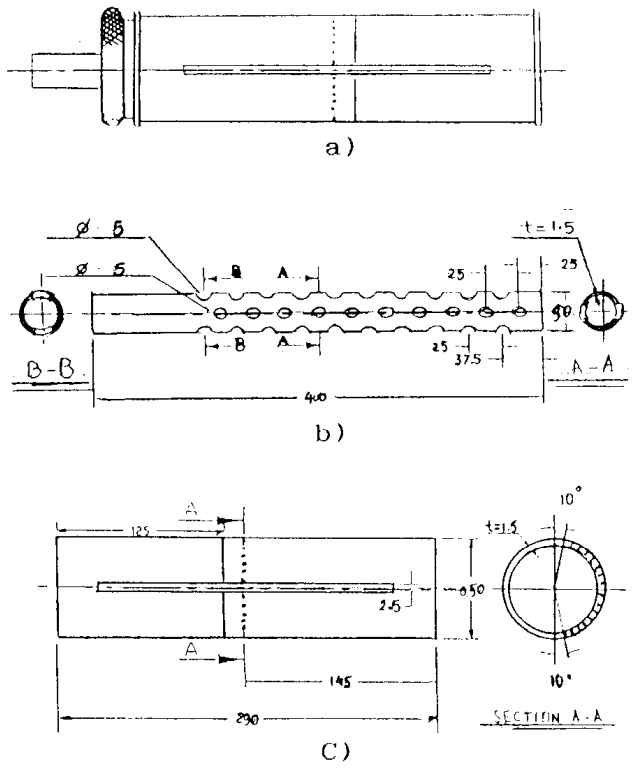

Figure 4. A schematic diagram of cylindrical model. **a**) Model, **b**) Brass Cylinder Insert, and **c**) Pressure Tappings Arrangement

RESULTS AND DISCUSSIONS

The location of injection slot from the leading edge was considered in three cases: 0, 10 and 20 degrees in the pressure side of the model. The flow chart of the experimental running is shown in Figure 5.

where, m° is the injected mass flow rate, α is the injection angle from leading edge in pressure side of blade and V_∞ is the main stream velocity. From the range of the main rate flows, Reynolds numbers based on cylinder diameter were under 10^5; therefore, the boundary layer over cylinder was in sub critical conditions [12]. By considering the injected rates, the cooling factor M (defined as the ratio of mass velocities $\rho_i V_i / \rho_\infty V_\infty$) was in the range of $0.1 < M < 3.9$.

In Figure 6 and Figure 7, the pressure distributions around cylinder are presented for the lowest and highest mainstream velocities (i.e., 5.7 m/s and 18 m/s) respectively. Other experimental conditions have also been inserted on the figure. For low main velocities, because of the strong diffusion of injected flow into the main one, the boundary layer over cylinder becomes unstable. Hence the pressure distribution is not regular and consequently, the effects of secondary flow on the hydrodynamics of recovery phenomena cannot be determined. The same results were obtained for all injection angles. Such a behavior has been observed for various main velocities up to 12 m/s. By further increase of the main flow velocity up to 12 m/s, it seems that the injected flow can not easily diffuse into the main flow because the injected flow mixes with the main flow very close to the injection slot. Therefore, in comparison with non-injected cases, the pressure distribution behaves in a regular manner for different injections. Figure 7 shows a sample results concerning this category in which the pressure distribution around the cylinder

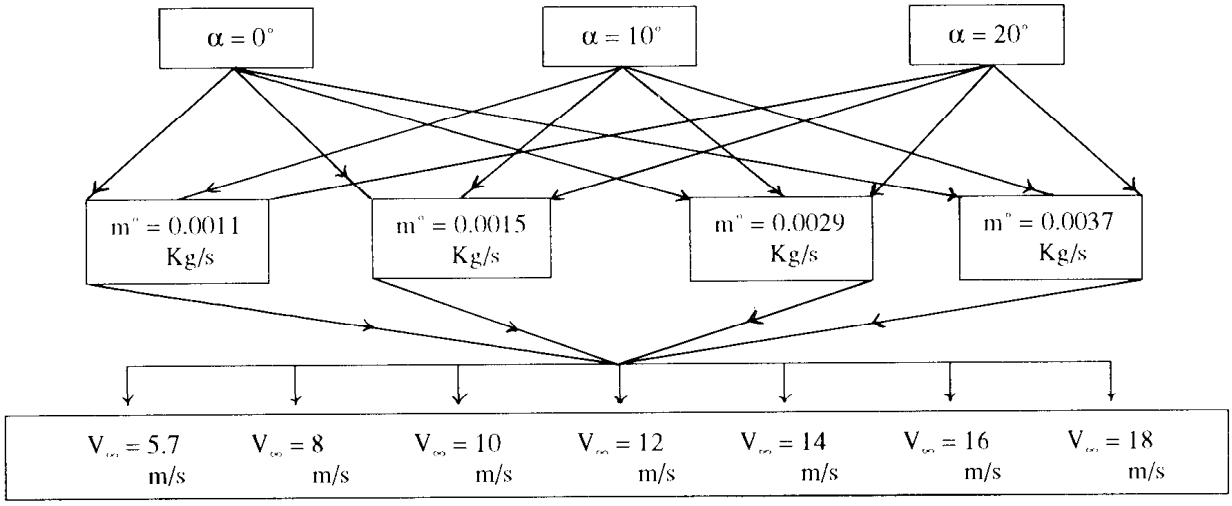

Figure 5. Flow chart of the experimental running.

was regularly affected by the injected mass flow rates.

There is also an intensive pressure drop just in the location of the slot while it starts to rise till around 20 degrees beyond the injection points. Therefore, it is possible to distinguish the region affected by the presence of the secondary flow. Beside this region, the behavior of pressure is the same as the case with no injection. That is, the secondary mass flow rates

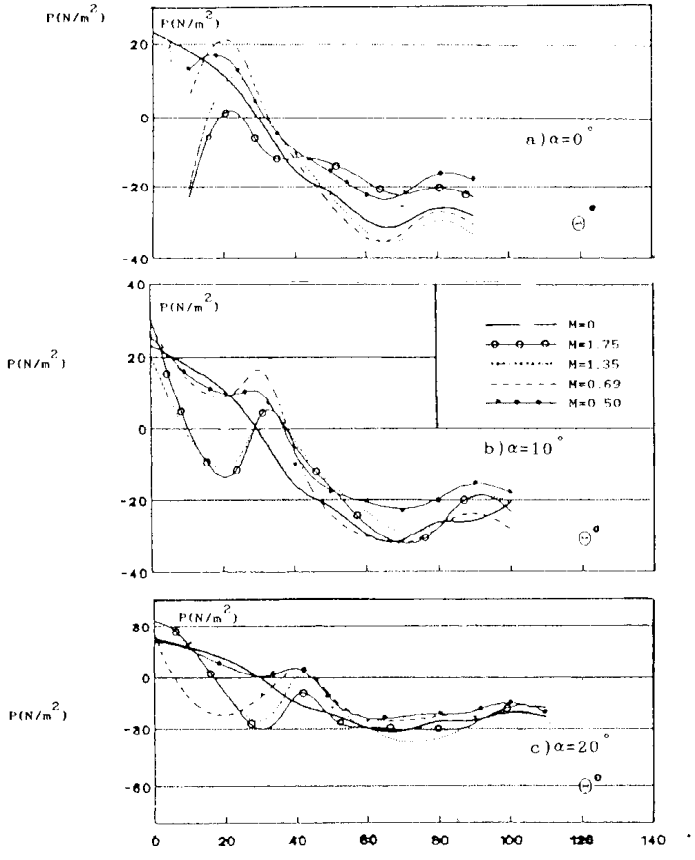

Figure 6. Pressure distribution on cylinder with and without injection. [V_∞ = 5.7 m/s, $R_e = 1.54 \times 10^4$]

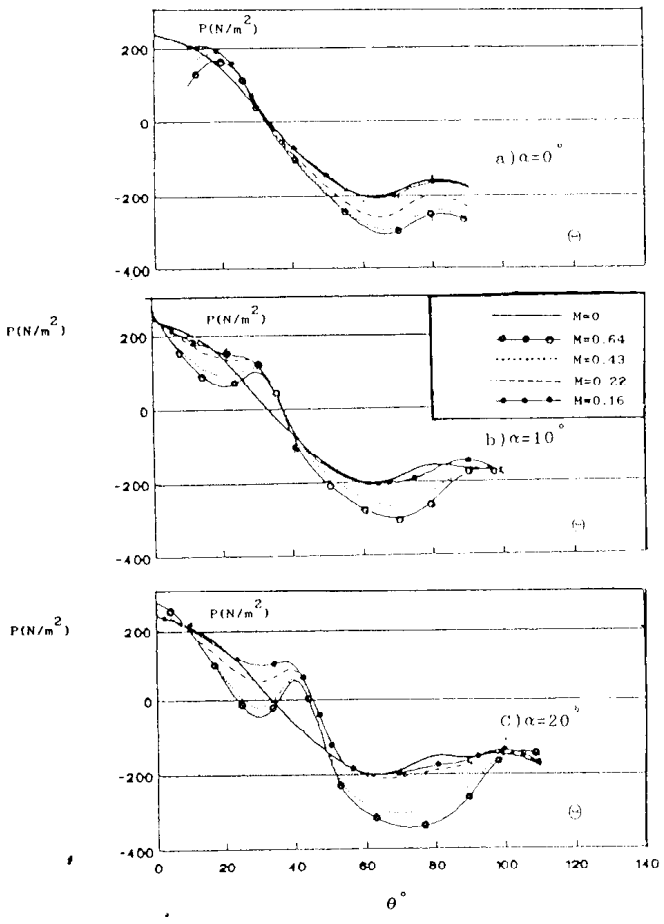

Figure 7. Pressure distribution on cylinder with and without injection. [V_∞ = 18 m/s, $R_e = 4.88 \times 10^4$]

causes more flow acceleration. The reason for an intensive decrease of pressure in the slot locations is simply the entrance of secondary flow into the boundary layer and blowing it off on the cylinder surface. Theoretical evidence indicates that the laminar boundary layer on a surface with non pressure gradient or with small negative pressure gradients "blows up" the surface when the blowing rate is [16]:

$$M > (v_\infty / V_\infty x)^{1/2}$$

where in x denotes the curvilinear distance from leading edge. Therefore, for all experimental running in the slot location, the boundary layer has been blown off by injected flows and the onset of the first separation region is located around this point. The increase of pressure in the close downstream region of slot depends on the interaction between shear flows. The main flow on having the high dynamic heads prevents the extend of separated region caused by secondary flow and locally stops it. So the boundary layer reattaches to the surface of the cylinder and the behaviors of flow become similar to no injection case. To understand this phenomenon, the case of α = 20 degrees has been taken. The ideal velocity distribution in potential irrotational flow past a circular cylinder of diameter d and free-stream velocity V_∞ can be presented as follows:

$$V(x) = 2\ V_\infty [2x / d - 1/6 ((2x / d)^3)]$$

where x denotes the distance between injection point and leading edge of the cylinder. From analytical calculation of Schlichting [12], the thickness of boundary layer in the point of injection i.e., α=20 degrees) when V_∞ = 18 m/s, is around 0.2 mm. The mean velocity of this shear layer becomes approximately 10 m/s. In the injection point the direction of secondary flow is normal to the surface, so for each experimental case (0.1 < M < 0.6 for example in the Figure 8), the velocity of injection is so high which affects the boundary layer and leads to a separation. In the closed downstream of injection, for external potential flow, the variation of stream wise velocity is not important while for injected flow the variation of velocity with θ is considerable. As it is seen from Figure 8, there is a favorite pressure gradient in the closed downstream of injection. So in this region there is an intensive action of secondary flow in changing the direction of outer potential flow. Then, with unfavorable pressure gradient, the velocity of injected layer progressively decreases with θ and the main velocity of potential flow becomes important. Finally, the injected layer is completely stopped by the action of external layer when the boundary layer reattaches the surface of cylinder. The separated region due to the presence of injected film, called "the first separation region (FSR) of the boundary layer, (to distinguish from the main separation over the cylinder caused by pressure grarients)" is very important for protecting the direct contact of main flow with the cylinder surface. This phenomenon has been already introduced by Fitt et al [8], but for slot injections with no pressure gradients.

In the present work the injection slot is located at the leading edge. FSR in divided in two parts, one in

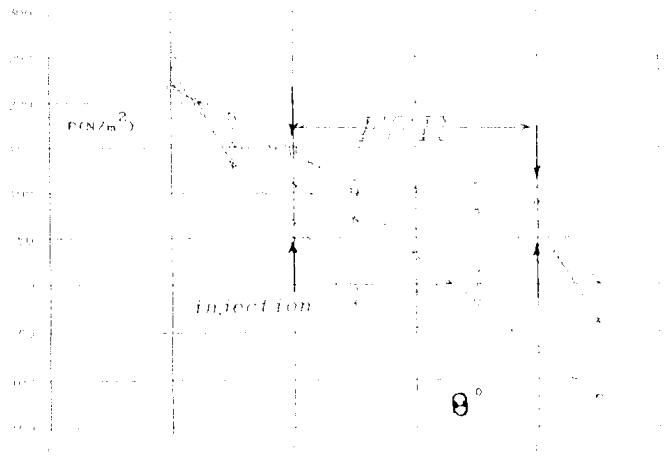

—□— M = 0 —+— M = 0.54 —○— M = 0.43 —Δ— M = 0.22 —×— M = 0.46

Figure 8. Representation of FSR in the case of α = 20

the pressure side and the other in the suction side. Based on this approval, its extends are seen from the curves smaller than the two others (i.e. 10 and 20 degrees after leading edge). The figures, also show that the length of FSR (distance from the injection slot to the end of unfavorable pressure gradients. Figure 8) is increased when the cooling factor and the injection angle increase. It is concluded that the FSR extends around 20 degrees after injection positions. Therefore, the single slot film cooling method may be used for local protection of surface from the direct contact of the main flow.

Clearly in order to determine the accurate location of the first separation region, it is required that not only the pressure distributions but the mean velocity field be measured. The advanced numerical methods can be used to predict the flow field. Many attempts have been made but only for very simple cases [13-16]. Nevertheless, when there are high pressure drops in the fields, the first step is to gain information about the pressure distributions. Its behaviors can be predicted only using the FSR phenomenon. For this reason, 10 and 20 degrees after slot have been considered for the rest of discussion.

The results for 10 degrees after slot, are represented in Figure 9, wherein the pressure coefficients $C_{P(10)}$ is plotted as a function of cooling factor M.

By definition:

$$C_{P(10)} = (P_{10} - P_\infty) / 0.5\, \rho_\infty v_\infty^2 \text{ and } M = \rho_j V_j / \rho_\infty V_\infty$$

where P_{10} denotes the gage pressure 10 degrees after slot.

All curves indicate that the pressure drops continuously increase with the cooling factor up to its maximum value. It may be interpreted that for each cooling factor, there is a critical case where the values of M less than this case have significant affects on the film cooling applications.

In the case of 20 degrees after slot, the pressure

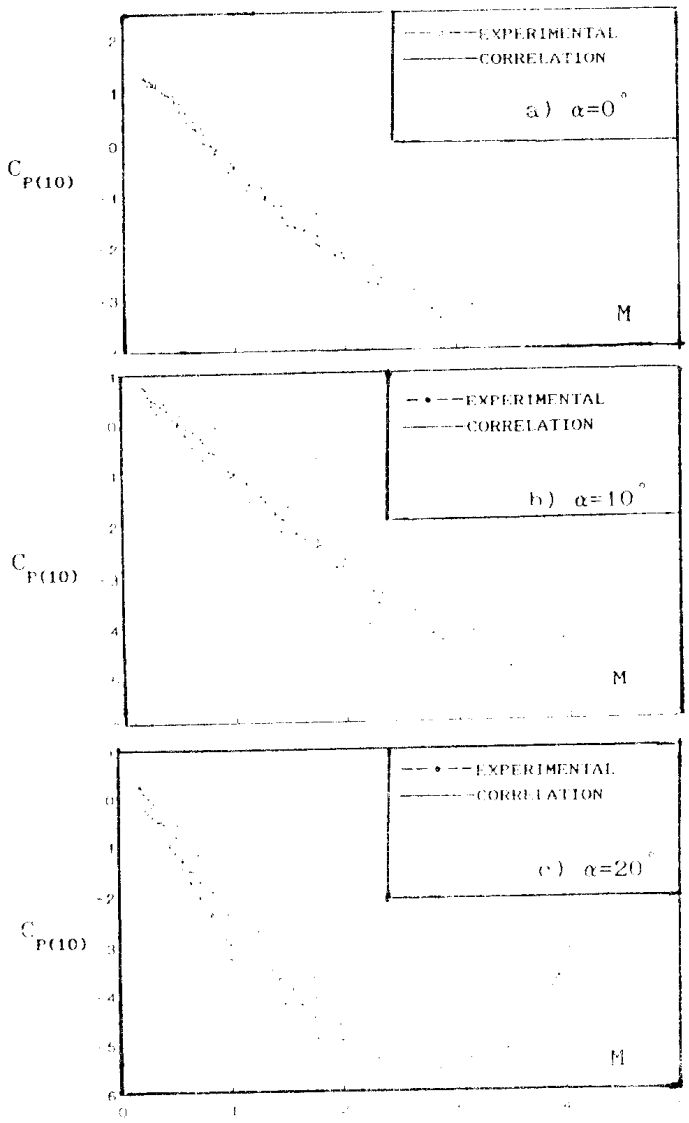

Figure 9. Pressure coefficient versus cooling factor for 10° after injection.

drops exhibits the behavior similar to the previous case, but for the same cooling factors the values are small because of the influence of the main pressure gradient. Therefore, by increasing the distance from injection slot, the main pressure gradients increase their velocities also increase. So, the velocity of injected flow decreased until it attaches the surface, then by strong recirculation of boundary layer the mixing of two shear layers occurs.

From the experimental data, the correlations for prediction of the pressure coefficients in the first separation regions were obtained by the least square polynominal approximation. These correlations and

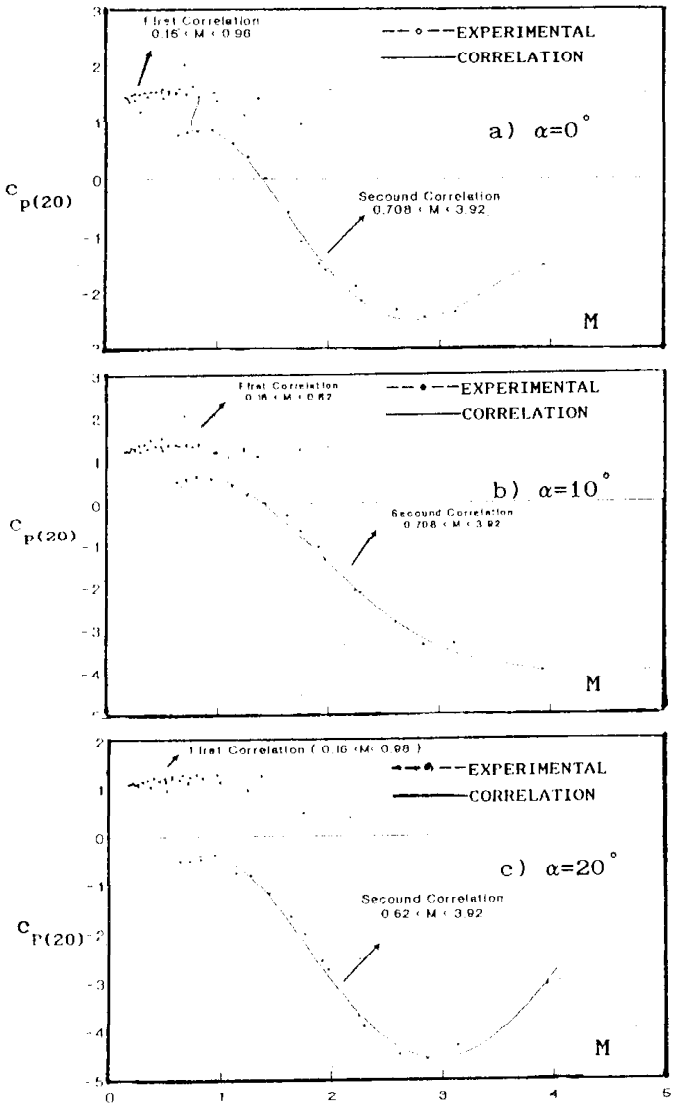

Figure 10. Pressure coefficient versus cooling factor for 20° after injections.

their maximum errors are shown in the Table 1.

CONCLUSIONS

The hydrodynamics behaviors of injected air flow at different angles, close to the leading edge of a horizontal cylinder have been studied using slot *film cooling* method. The prediction of full coverage film cooling, on the pressure side of the cylinder with recognition of a first separation region of the boundary layer, has been achieved. The results show that the first separation domain extends with increasing the *blowing factor* until around 3. For the M larger than this limit, the secondary flow influences strongly the main flow by increasing the instability of the boundary layer. This leads to the mixing of the two flows.

The first separation region (FSR) is concentrated on the slot location and its closed downstream. Therefore, only the local protection is possible in this method. However, for a detailed prediction of (FSR), the velocity field of two shearing flows in the domain of fluid injection must be known by measuring the distribution of the two dimensional components of the velocity.

Clearly, with recognition of the (FSR) location, the effectiveness of film cooling can be improved by

TABLE 1. Experimental Correlations of $C_P = f(M)$

$C_{P10} = f(M)$ for 10° after slot in the range of $0.16 < M < 4$		
θ (injection angles)	**CORRELATION**	**Max. error**
0°	$C_{P10} = 1.64-2.11M-0.20M^2+0.13M^3-0.01M^4$	10%
10°	$C_{P10} = 0.99-1.82M-0.26M^2+0.06M^3+0.01M^4$	17%
20°	$C_{P10} = 1.45-6.93M+3.68M^2-1.19M^3+0.16M^4$	16%
$C_{P20} = f(M)$ for 20° after slot in the range of $0.6<M<4$		
θ (injection angles)	**CORRELATION**	**Max. error**
0°	$C_{P20} = -3.66+12.67M-11.35M^2+3.45M^3-0.34M^4$	10%
10°	$C_{P20} = -3.01+9.38M-7.64M^2+2.03M^3-0.18M^4$	6%
20°	$C_{P20} = -4.86+11.96M-10.02M^2+2.74M^3-0.23M^4$	5%

heat transfer measurements.

ACKNOWLEDGMENTS

The author wishes to record his sincere thanks to Professor K. Suzuki and Associate Professor Y. Hagiwara from Kyoto University for their direct and indirect contributions to this work. The assistance of Mr. G. Khalagi from Department of Mechanical Engineering of Tabriz University in the execution of some parts of the experimental work is also acknowledged.

NOMENCLATURE

$C_{P(10)}$	pressure coefficients 10° after slot
$C_{P(20)}$	pressure coefficients 20° after slot
d	diameter of cylinder and orifice
D	diameter of secondary flow line
FSR	first separation region
h	difference pressure in height of liquid manometer
M	cooling factor
m°	mass flow rate
P_{10}	gage pressure 10° after slot
P_{20}	gage pressure 20° after slot
P_∞	wind tunnel gage pressure
R_e	Rynolds number based on cylinder diameter
R_{eD}	Rynolds number based on pipe diameter of the injection
T_{aw}	adiabatic wall temperature
T_i	injected flow temperature
T_∞	main flow temperature
V_i	injected flow velocity
V_∞	mainstream velocity
x	stream wise coordinate

Greeks

α	slot angle from leading edge
β	ratio of orifice to pipe diameters
ε	air secondary flow compressibility factor
ν	kinematic viscosity of fluid
ρ	density of fluid
θ	location of pressure taps from leading edge in degree
η	effectiveness of film cooling

Subscripts

i	denotes the injected flow
∞	denotes the main flow

REFERENCES

1. M. M. El. Wakil, "Power Plant Technology." McGraw Hill, N. Y., (1988).
2. B. Barry, "The Aerodynamic Penalties Associated with Blade Cooling. In Turbine Blade Cooling"; VKI LS 83, (1976).
3. R. J. Goldstein, "Film Cooling. Advanced in Heat Transfer", Academic Press, N. Y. & London, (1971), pp 321-379.
4. R. P. Bring et al, "Experimental Investigation of Film Cooling on Turbine Rotor Blade." *J. Egg. for Power., ASME* Vol. 100, July (1978).
5. R. P Bring et al, "Film Cooling of a Gas Turbine Blade." *J. Egg. for Power., ASME,* Vol. 102, N. 1 Jan. (1980) pp 81-87.
6. Von Karman Institute for Fluid Dynamic, "Film Cooling and Turibine Heat Transfer". Lecture Series; Vol. 1 and Vol. 2, (1982).
7. K. Takers et al, "Experimental Study of Heat Transfer and Film Cooling on Low Aspect Ratio Turbines Nozzles". *J. Turbomach.;* Vol. 112, N. 2, Jul. (1990), pp 448-496.
8. A. D. Fitt et al, "Aerodynamics of Slot Film Cooling: Theory and Experimental". *J. Fluid Mech.,* Vol. 160, (1985), pp 15-57.
9. S. G. Schwarz et al, "Influence of Curveture on Film Cooling Performance". *J. Turbomach.;* Vol. 113, N. 3, Jul. (1991), pp 472-478.

10. A. J. H. Teekaran et al, "Film Cooling in the Presence of Mainstream Pressure Gradients". Int. Gas Turbine and Aeroengine Congress; Jun. Brussel, Belgium, (1990).
11. N. Kasagi et al, "Effects of the Wall Curvature on the Full-Coverage Film Cooling Effectiveness". First int. Sym. on Transport Phenomena, Honolulu, USA, May, (1985).
12. H. Schlichting, "Boundary Layer Theory. McGraw Hill, N. Y. (1979).
13. S. Yavuzkurt et al, "Full Coverage Film Cooling: 2-Prediction of the Recovery Region Hydrodynamics". *J. Fluid Mech.*, Vol. 13, N. 101, (1980), pp 159-178.
14. T. R. Shembharkar et al, "Prediction of Film Cooling with a Liquid Coolant. "*Int. J. Heat Mass Transfer*; Vol. 29, N. 6, Jun, (1986) pp 899-908.
15. I. Gartshore et al, "Film Cooling Effectiveness". *Trans. Can. Soc. Mech. Eng.*, Vol. 15, N. 1, (1991) pp 43-56.
16. J. D. Cole and J. Aroesty, "The Blowhard Problem Inviscid Flows with Surface Injection"; *Int. J. Heat Mass Transfer*, Vol. 11 (1968) pp. 1167-1183.